https://doi.org/10.1016/j.resconrec.2022.106254

Performance of Zeolite Synthesized from Sewage Sludge Ash as a Warm Mix Asphalt Additive

Fuliao Zou [a,1], Zhen Leng [a,2*], Ruijun Cao [a,3], Gaoyang Li [a,4], Yuan Zhang [b,5], Anand Sreeram [c,6]

[a] Department of Civil and Environmental Engineering, The Hong Kong Polytechnic University, Hung Hom, Kowloon, Hong Kong

[b] School of Civil Engineering and Transportation, South China University of Technology, Guangzhou, Guangdong, China

[c] Department of Civil, Architectural and Environmental Engineering, The University of Texas at Austin, Austin, Texas, United States of America

Abstract

The disposal of sewage sludge ash (SSA) is a growing problem with both environmental and economic ramifications. This study aims to synthesize zeolite from SSA as a foaming-based warm mix asphalt (WMA) additive, and comprehensively characterize its performance. The SSA-derived zeolite was first characterized using X-ray Diffractometer (XRD), Scanning Electron Microscope (SEM), and Thermogravimetry-Differential Thermal Analyzer (TG-DTA) tests. Then, WMA mixtures with the SSA-derived zeolite and a commercial zeolite additive, and a conventional hot mix asphalt (HMA) mixture were produced in the laboratory for a wide range of engineering performance tests, including the indirect tensile stiffness modulus test, indirect tensile fatigue test, moisture susceptibility test, and Hamburg wheel-tracking test. The experimental results indicated that the SSA-derived zeolite was pure zeolite A which can release approximately 20% crystal water gradually from 70 ºC to 200 ºC. The overall performance of the WMA mixture with SSA-derived zeolite was better than that of the WMA mixture with commercial additive, and comparable to that of the HMA mixture except for rutting resistance, which is marginally lower but still satisfactory. Cost-benefit analysis was conducted in the end, which demonstrated that SSA-derived zeolite is eco-efficient. This study concluded that it is feasible to use the SSA-derived zeolite as an effective and sustainable WMA additive.

Keywords: Sewage Sludge Ash, Zeolite Synthesis, Warm Mix Additive, Chemical Property, Asphalt Mixture Performance, Cost Analysis

[1] PhD Candidate, fu-liao.zou@connect.polyu.hk

[2]* Associate Professor, Tel: +852-2766-6007; Fax: 852-2334-6389; Email: zhen.leng@polyu.edu.hk (*Corresponding Author)

[3] Post-Doctoral Fellow, ruijun.c.cao@connect.polyu.hk

[4] PhD Student, 21064985r@connect.polyu.hk

[5] Post-Doctoral Fellow, yuanzhang@scut.edu.cn

[6] Post-Doctoral Fellow, anand.sreeram@austin.utexas.edu

1. Introduction

Warm mix asphalt (WMA) is a green paving technology that reduces the construction temperature of asphalt mixtures without compromising their overall engineering performance (Leng et al., 2014). Depending on the technology used in producing WMA, the construction temperature of the conventional hot mix asphalt (HMA) pavement can be lowered by about 20-40 ºC (Capitão et al., 2012; Rubio et al., 2012). This temperature reduction can be achieved by using organic additives, chemical additives, and foaming technologies (Kheradmand et al., 2014; Xiao et al., 2011; Yu et al., 2018). In practice, foaming-based warm mix technology appears to be preferred because of its lower cost and simple operation (Middleton and Forfylow, 2009). The foaming process can be accomplished by either direct water injection through a nozzle or by adding foaming additives, such as zeolites containing crystal water in their micropore structure. When zeolites are added into the asphalt mixture at construction temperatures, the crystal water is released and vaporized, resulting in a rapid volume expansion or foaming of the asphalt binder, which can improve the workability of asphalt mixtures and increase aggregate coating at lower manufacturing temperatures. Both natural zeolites (e.g., clinoptilolite) and commercial synthetic zeolites (e.g., Aspha-min, Advera) have been employed to produce WMA mixtures. It was reported that the commercial synthetic zeolites can promote a better distribution of the binder within the asphalt mixture and improve the compactability of asphalt mixtures without negatively affecting the engineering performance (Kristjánsdóttir et al., 2007; Woszuk and Franus, 2017). Natural zeolites can be considered as an alternative WMA additive to commercial synthetic zeolites due to their additional economic and environmental benefits (Sengoz et al., 2013; Valdes et al., 2018). Studies have also indicated that zeolites can be synthesized from sewage sludge ash (SSA), a waste product commonly landfilled with growing environmental apprehension (Environmental Protection Department, 2020), which offers a potential value-added approach to recycle waste materials into WMA additives.

The management and disposal of sewage sludge from sewage treatment works has become a global issue generating increasing environmental and economic concerns in high population density cities around the world (Lam et al., 2015). Currently, sewage sludge is commonly subjected to energy-intensive dewatering process and incineration, followed by disposal at local landfill sites due to a lack of sustainable recycling approaches. With limited land resources and the capacity of local recycling, there is a growing demand for novel approaches for the sustainable treatment of sewage sludge. Recent studies have investigated the utilization of SSA in cementitious materials and heavy metals adsorbent materials (Benassi et al., 2019; Wang et al., 2018a; Zhou et al., 2020). It was reported that the particle sizes of SSA can range from submicron to around 700 μm (Cyr et al., 2007). The exact contents of the major elements and the amorphous glassy phases of SSA depend on the sludge treatment processes applied at wastewater plants, as well as other factors such as industrial activities and the types of sewerage system in the catchment area (Anderson and Skerratt, 2003; Wiebusch and Seyfried, 1997).

Nonetheless, the major components in SSA are Si, Al, Ca, Fe, P, and Na (Cyr et al., 2007; Mahieux et al., 2010). Common crystalline forms of these elements are inert quartz (SiO_2), magnetite (Fe_3O_4), anorthoclase ($(NaK)Al{\cdot}Si_3O_8$), and whitlockite ($Ca_3(PO_4)_2$) (Donatello and Cheeseman, 2013; Zhang et al., 2018). It is interesting to note that synthetic zeolites may be produced from SSA, as zeolites are microporous hydrated aluminosilicates that mainly consist of elements Al and Si (Cardoso et al., 2015; Kim and Lee, 2009). Among various types of zeolites, Zeolite Linde Type A (Zeolite LTA or Zeolite A) presents beneficial commercial characteristics that include thermal stability, high selectivity, and non-toxicity (Qian and Li, 2015). Moreover, it can gradually release its crystalline water between 100 ^{o}C to 200 ^{o}C, which was found the most suitable for being applied as a WMA additive (Afzal et al., 2000; Woszuk and Franus, 2017). The general formula for zeolite A is $Na_{12}[(AlO_2)_{12}(SiO_2)_{12}]\ 27H_2O$ wherein the framework silicon to aluminum (Si/Al) ratio is close to one in most cases, and sodium ions are the exchangeable extra-framework cations (Collins et al., 2020). The zeolite synthesis from loam minerals and waste materials containing Si and Al sources (e.g., kaolin, fly ash, and SSA) by the hydrothermal reaction consists of three steps (Rios et al., 2009; Murayama et al., 2002): the dissolution of Si and Al, the condensation of silicate and aluminate ions in alkali solution to make aluminosilicate gel, and the crystallization of aluminosilicate gel to make zeolite crystal. A method was proposed to convert SSA to zeolite and apply it as a WMA additive for asphalt pavement (Zhang et al., 2018). The alkaline fusion of SSA with the sodium hydroxide (NaOH), followed by the hydrothermal reaction on the alkaline solution of the fused product was conducted to synthesize the target zeolite. The produced SSA-derived zeolite was used as a foaming additive for manufacturing the WMA mixture. The findings indicated that SSA-derived zeolite has a high potential to be used as a WMA additive, and it has a similar temperature reduction function as the commercial synthetic zeolite Aspha-min. However, the chemical characteristics of SSA-derived zeolite and performance properties of the WMA mixture with SSA-derived zeolite are still unknown. Since there are concerns about moisture susceptibility and rutting resistance for WMA mixtures with zeolite additives (Hasan et al., 2015; Xu et al., 2017), it is necessary to comprehensively study the engineering performance of WMA mixtures with SSA-derived zeolite for practical applications. Moreover, although the synthesis of SSA-derived zeolite removes SSA from landfilling, the economic efficiency of the synthesis process has not been evaluated. Therefore, the main objectives of this study are to investigate the performance of the WMA mixture with SSA-derived zeolite through comprehensive laboratory tests, compare the results with the WMA mixture prepared using Aspha-min and conventional HMA mixture, and characterize the cost-effectiveness of applying SSA-derived zeolite as a WMA additive.

2. Research Materials and Methodology

2.1. Raw materials

Three types of mixes were prepared in this study, namely conventional HMA, warm mix asphalt with SSA-derived zeolite (WMAZ), and warm mix asphalt with Aspha-min (WMAA). The dosage of Aspha-min was 0.3% by the total mass of the asphalt mixture, which is recommended by the supplier and commonly applied in practice. The same dosage was used for the SSA-derived zeolite. All three mixtures shared the same mixture design, which was the polymer

modified stone mastic asphalt with a nominal maximum aggregate size of 10 mm (PMSMA10), a surface course material for carriageway pavements commonly used in Hong Kong (Highways Department, 2020). Styrene-Butadiene-Styrene (SBS) polymer modified bitumen that has a Superpave performance grade of PG76-16 was used as the asphalt binder (AASHTO M320-10, 2013). The binder content was 6.0% by the total mass of the asphalt mixture. Local granite rocks were used as the coarse and fine aggregates, as well as the mineral filler. Cellulose fiber and hydrated lime were also used in the PMSMA10 mixtures according to local requirement. The cellulose fiber content was 0.3% by the total mass of the asphalt mixture. The gradation of PMSMA10 is presented in **Table 1**.

Table 1 Gradation of the PMSMA10 mixture

Composition	Bulk specific gravity	Sieve size (mm)	Percentage (%)
Coarse aggregates	2.642	14-10	3.5
	2.663	10-5	59.5
	2.709	5-2.36	9.0
Fine aggregates	2.649	2.36-0.075	16.5
Mineral filler	2.661	<0.075	9.5
Hydrated lime	2.587		2.0

2.2. Synthesis of SSA-derived zeolite

SSA contains large percentages of silicon dioxide and aluminum oxide which can be used as source materials for the synthesis of zeolite. SSA-derived zeolite was synthesized based on the following procedure: SSA was first activated through the process of alkaline fusion using 500 g SSA and 575 g NaOH at 500 ºC for 1 h. Then, the fused product was dissolved in the NaOH solution with a concentration of 2.5 mol/L at 65 ºC for 3 h. Afterward, the sodium aluminate ($NaAlO_2$) powder was added to the supernatant solution to adjust the molar ratio of Si/Al to 0.8. The product was crystallized at a temperature of 80 ºC for 3 h and filtered out to obtain a white powder. Using this method, pure zeolite A, a suitable type of zeolite for WMA additives, can be synthesized from SSA. The process to produce zeolite from SSA is illustrated in **Fig. 1**. The SSA used to produce SSA-derived zeolite was provided by the sludge treatment facility (T-Park) in Tuen Mun, Hong Kong.

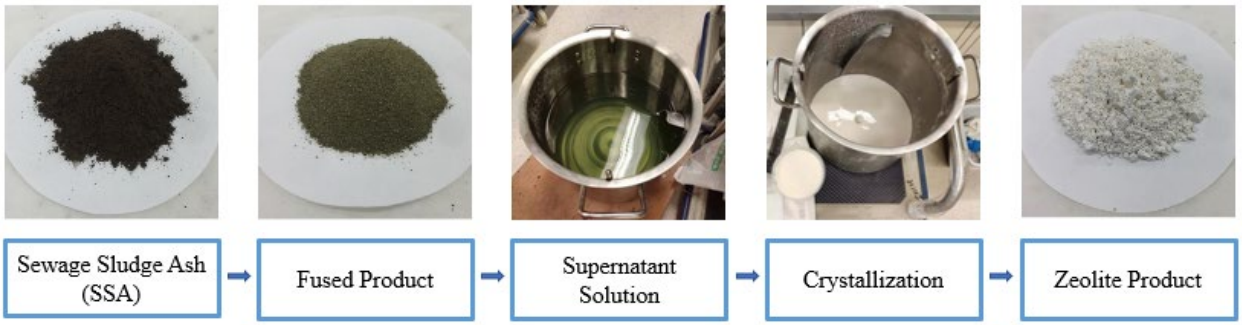

Fig. 1. Synthesis of zeolite from SSA

2.3. Characterization of SSA-derived zeolite

X-ray Diffractometer (XRD) test, Scanning Electron Microscope (SEM) test, and Thermogravimetry-Differential Thermal Analyzer (TG-DTA) test were conducted to characterize the chemical and physical properties of the two zeolite-based WMA additives. Rigaku SmartLab X-ray Diffractometer equipped with a 9-kW rotating anode X-ray source with a high-quality semiconductor detector was used to identify the crystalline phases of the WMA additives. An X-ray wavelength (λ) of 1.54 Å, a scanning step width of 0.02°, and a scanning speed of 4° /min were used in this study. Rigaku's PDXL software was used to compare the detected XRD patterns with the standard patterns from the powder diffraction file (PDF) database. Tescan VEGA3 SEM system that has a maximum magnification of 100,000X was used to characterize the morphology of WMA additives. Gold sputtering coatings were applied on the WMA additives before the SEM tests. Rigaka Thermo plus EVO2 thermal analyzer was used to determine the thermal properties of WMA additives. During the TG-DTA tests, the WMA additives were heated from 25 °C to 500 °C at a heating rate of 10 °C/ min.

2.4. Mixture specimen preparation

The HMA mixture was mixed at 180 °C and compacted at 160 °C. The WMA mixtures were mixed at 155 °C and compacted at 135 °C. Superpave Gyratory Compactor (SGC) was used to produce test specimens. The air void contents of the produced specimens were 4% ± 0.5% for the Indirect Tensile Stiffness Modulus (ITSM) and Indirect Tensile Fatigue (ITF) tests. The air void contents of the produced specimens were 7% ± 0.5% for the moisture susceptibility test and the Hamburg wheel-tracking test. Three replicate specimens were prepared and tested for each test except for the Hamburg wheel-tracking test, which used two replicate specimens. The general information on the tests and the prepared specimens is summarized in **Table 2**.

2.5. Laboratory tests for engineering performances

Asphalt pavements are prone to surface distresses such as fatigue cracking, moisture damage, rutting, and thermal cracking under heavy traffic loading (Jiang et al., 2020; Li et al., 2020;

Wang et al., 2018b). Since the local climate in Hong Kong is relatively hot and humid, this study focused on the intermediate temperature durability and high temperature performance of the produced asphalt mixtures. The ITSM and ITF tests were conducted to investigate the cracking resistance of the produced asphalt mixtures at intermediate temperatures. The freeze-thaw cycle conditioned moisture susceptibility test was conducted to evaluate the moisture susceptibility of the produced asphalt mixtures. The immersion Hamburg wheel-tracking test was conducted to investigate the rutting resistance of the produced asphalt mixtures under high temperature and humidity.

2.5.1. ITSM and ITF tests

Test specimens with a diameter of 100mm and a thickness of 40mm were produced for the ITSM test and ITF test, according to BS DD 213 (1993) and BS EN 12697-24 (2012), respectively. The ITSM test was conducted on both unaged and aged specimens to evaluate the differences in stiffness modulus before and after aging. The aged specimens were subsequently used to run the ITF test. The ITF test was conducted under the stress-controlled mode at three stress levels. The aged specimens were produced according to AASHTO R30-02 (2010), in which the loose mixtures were conditioned in a force-draft oven for 4 h at 135 ºC for short-term aging and then compacted and aged in the oven for 5 days at 85 ºC.

2.5.2. Moisture susceptibility test

Test specimens with a diameter of 100mm and a thickness of 62.5mm were produced for the moisture susceptibility test, according to ASTM D4867-09 (2014). The Tensile Strength Ratio (TSR) between the mixtures with the freeze-thaw cycle conditioning and the mixtures without the freeze-thaw cycle conditioning was measured to evaluate the moisture susceptibility. The specimens conditioned with freeze-thaw cycle were partially saturated with water and conditioned in a freezer at -18 ºC for 16 h and then in a water bath at 60 ºC for 24 h. The Dynamic Testing System (DTS-30) from PAVETEST was used for measuring the ITSM, ITF, and TSR.

2.5.3. Hamburg wheel-tracking test

Test specimens with a diameter of 150mm and a thickness of 60mm were produced for the Hamburg wheel-tracking test, according to AASHTO T324-11 (2013). The Immersion Wheel Tracker (CRT-WTIM) from Cooper Research Technology equipped with a moving steel wheel, a water bath, and a linear variable differential transducer system for measuring the rut depth was used for this test. During the test, the specimens were submerged in water and subjected to a steel wheel loading with a rolling speed of 52 passes/min. The water temperature can be set from 25 ºC to 70 ºC, with 50 ºC being the most common test temperature, which was used in this study. Except for running the test at 50 ºC, a water temperature of 60 ºC was also chosen in this

study to investigate the high temperature performance of produced HMA and WMA mixtures. Rut depth was measured at every 200 passes of the wheel and a maximum of 20,000 passes was applied for each test.

Table 2 General information of the tests and specimens

Test	Mixture	Mixing/ compaction temperature (°c)	Specimen diameter/ thickness (mm)	Air void content (%)	Test temperature (°c)	Condition
Indirect tensile stiffness modulus	HMA	180/ 160	100/ 40	3.5 - 4.5	20 ± 0.2	Unaged & aged
	WMAZ	155/ 135				
	WMAA					
Indirect tensile fatigue	HMA	180/ 160	100/ 40	3.5 - 4.5	20 ± 0.2	Aged
	WMAZ	155/ 135				
	WMAA					
Moisture susceptibility	HMA	180/ 160	100/ 62.5	6.5 - 7.5	25 ± 0.5	Unaged
	WMAZ	155/ 135				
	WMAA					
Hamburg wheel-tracking	HMA	180/ 160	150/ 60	6.5 - 7.5	50 ± 1.0 & 60 ± 1.0	Unaged
	WMAZ	155/ 135				
	WMAA					

2.6. Cost-benefit analysis

After characterizing the engineering performance of the WMA mixture prepared with SSA-derived zeolite, a cost-benefit analysis was conducted to quantify the cost-effectiveness of the synthesis process of SSA-derived zeolite. It is worth noting that producing 1 kg zeolite would also generate 1.18kg mineral filler as a by-product, which could replace part of the filler required for preparing asphalt mixture. Therefore, in the cost-benefit analysis, the cost mainly covered the input material and energy cost, and the benefit was considered as the saving brought by the by-product from the synthesis process. **Table 3** lists the unit cost and quantity of the input items that produced 1kg zeolite. The energy use was evaluated as the electricity consumption measured in the lab during the synthesis treatment. The material cost was collected from the Chinese manufacturer suppliers, and the electricity cost was obtained from the China Light and Power Co Ltd based on the current energy structure in Hong Kong. The monetary values of all items have been converted to equivalent US dollars. For the benefit from the by-product, the cost evaluation result would largely depend on the corresponding filler type and the content it replaced.

According to the survey in relevant Chinese manufacturer suppliers, the unit cost of mineral filler ranged from $0.02 to $0.1 per kilogram depending on the varied recipes.

Table 3 Cost inventory of the synthesis process derived from SSA

Input items		Unit cost ($)	Quantity
Material	SSA	NA	1.53kg
	NaOH	0.01	0.14kg
	$NaAlO_2$	0.36	0.51kg
Energy	Electricity	0.16	3.11KWh

3. Results and Discussion

3.1. Characterization of SSA-derived zeolite

Fig. 2. shows the XRD patterns of SSA-derived zeolite and Aspha-min. It can be observed that SSA-derived zeolite had a XRD pattern very similar to that of the Aspha-min. Only a few differences in the peak locations with very low intensity can be found in the patterns, suggesting that SSA-derived zeolite had a very similar crystalline structure compared with Aspha-min. There were minor differences in the peak intensities, which indicates the grain size of these two materials are different. Comparing their XRD patterns with the standard patterns from the powder diffraction file database supplied by the International Centre for Diffraction Data (ICDD), it was found that only the crystalline phase of zeolite A was included in the SSA-derived zeolite. In Aspha-min, the major crystalline phase was also zeolite A. But some other unknown crystalline phases were also observed. Zeolite A has a three-dimensional pore structure with pores running perpendicular to each other in the x, y, and z planes. The pore diameter is defined by an eight-member oxygen ring and is small at 4.2 Å, which leads to a larger cavity of a minimum free diameter of 11.4 Å.

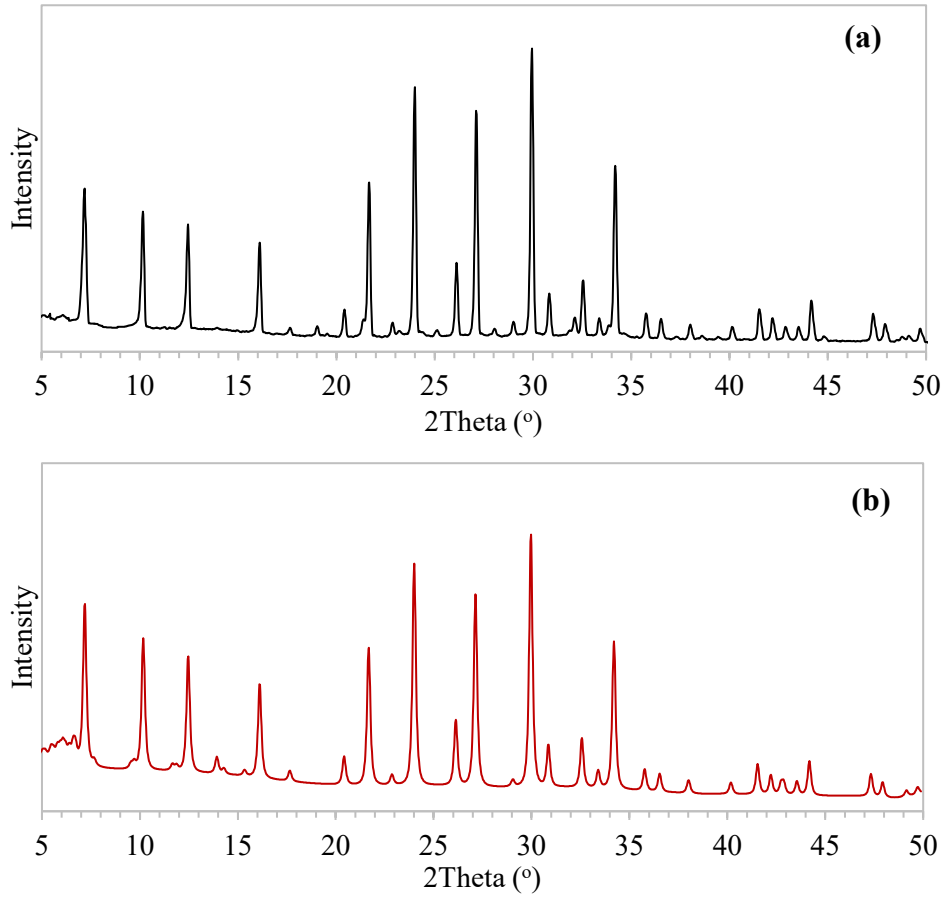

Fig. 2. XRD patterns of: (a) SSA-derived zeolite; and (b) Aspha-min

Fig. 3. shows the SEM images of the SSA-derived zeolite and Aspha-min. It is clear that both materials had a simple cubic crystalline structure. The difference between SSA-derived zeolite and Aspha-min was their grain size wherein SSA-derived zeolite had a smaller grain size. The SSA-derived zeolite had a crystalline size of about 1µm in diameter while the Aspha-min had a crystalline size of about 2µm in diameter. The chemical compositions of SSA-derived zeolite and Asphamin were determined by X-ray fluorescence (XRF) analysis. **Table 4** presents their chemical compositions in a form of major elements at weight percentages. The thermal properties of SSA-derived zeolite and Aspha-min are illustrated in **Fig. 4**. The weight loss over the range 25-200 °C confirms the release of water and the weight loss over the range 200-500 °C indicates the thermal decomposition and the release of the pyrolysis products (de Angelis Curtis et al., 1999; Duan et al., 2008; Saldo et al., 2002). It can be observed that both the SSA-derived zeolite and Aspha-min released crystal water when the temperature was increased, but Aspha-min had less weight loss and an earlier heat absorption peak than the SSA-derived zeolite. Aspha-min showed a weight loss of 20.5% while the observed weight loss from SSA-derived zeolite was 23.4%, which was 14% larger than that of the Aspha-min. The heat absorption peak was at 113 °C for Aspha-min while it was at 136 °C for the SSA-derived zeolite. The results indicated that SSA-derived zeolite can release more crystal water and the release is steadier when

heated. This is because SSA-derived zeolite has a higher Si/Al ratio (1.28) compared to Asphamin (1.19) (see **Table 4**). The water-binding force of zeolite is increased with the higher Si/Al ratio, which results in slower water release (Woszuk et al., 2017). Also, divalent cations (e.g., Mg^{2+} and Ca^{2+}) are more hydrated by water particles than monovalent cations. SSA-derived zeolite has a total amount of 0.78 wt % divalent cations, which is more than double compared to that of Asphamin (0.36 wt %). Moreover, SEM results confirmed the smaller grain size of SSA-derived zeolite compared to Asphamin, which results in a larger specific surface area and volume that contribute to a higher number of water-binding sites per mass unit. These characteristics determined the higher water binding ability and stronger water-binding force of SSA-derived zeolite, which results in an expected better foaming effect and asphalt coating of WMA mixtures with SSA-derived zeolite. Both the SSA-derived zeolite and Aspha-min started to release crystal water when heating begins, and the release became more significant at around 80 ºC and continued up to approximately 190 ºC, then, SSA-derived zeolite and Aspha-min slowly decomposed as temperature rises from 190 ºC to 500 ºC. The observed percentage weight losses of crystal water from both the SSA-derived zeolite and Aspha-min were approximately 20%.

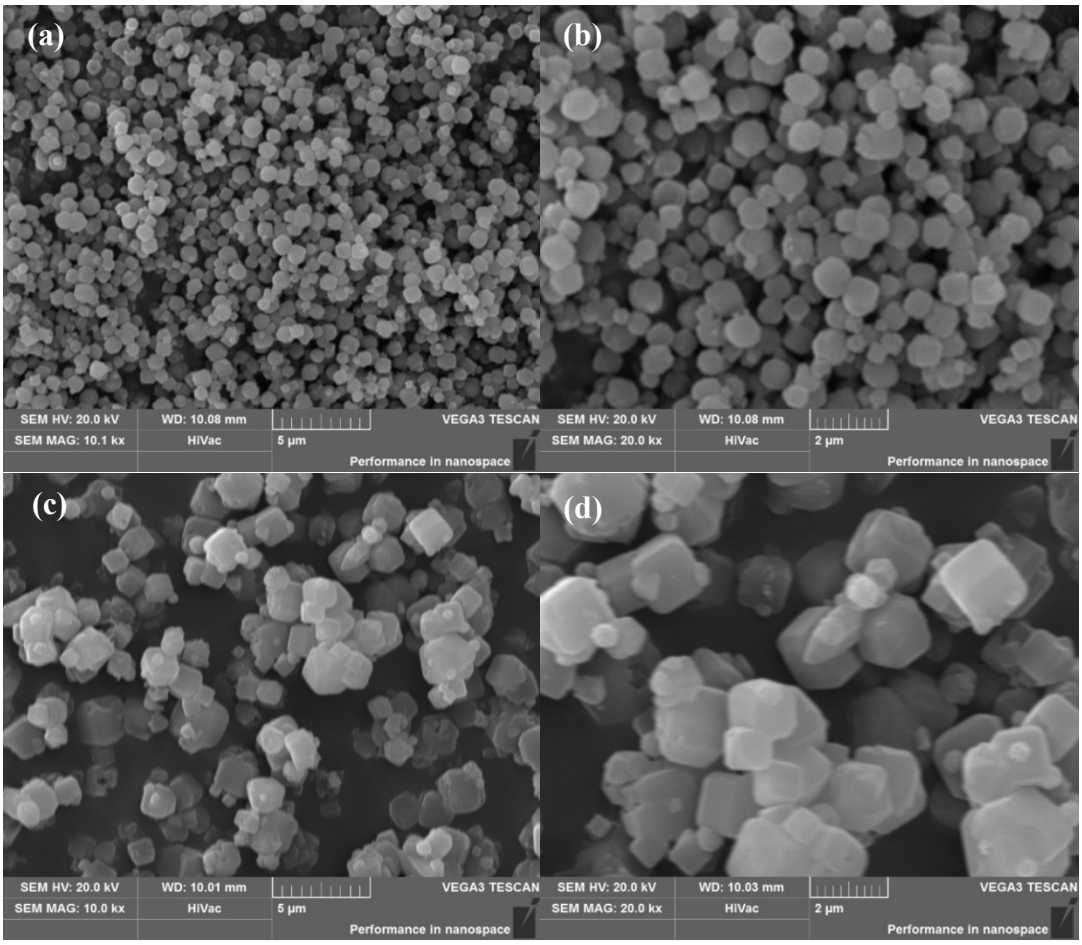

Fig. 3. SEM images of SSA-derived zeolite ((a) 10k× and (b) 20k×) and Aspha-min ((c) 10k× and (d) 20k×)

Table 4 XRF result of SSA-derived zeolite and Asphamin illustrating the quantities (wt %) of major elements.

Component	SSA-derived Zeolite (wt %)	Asphamin (wt%)
Na	20.00	22.60
Mg	0.26	0.27
Al	33.80	32.40
Si	43.10	38.60
P	0.12	0.08
S	0.17	5.15
Cl	0.08	0.48
K	1.15	0.23
Ca	0.52	0.08
Fe	0.71	0.07

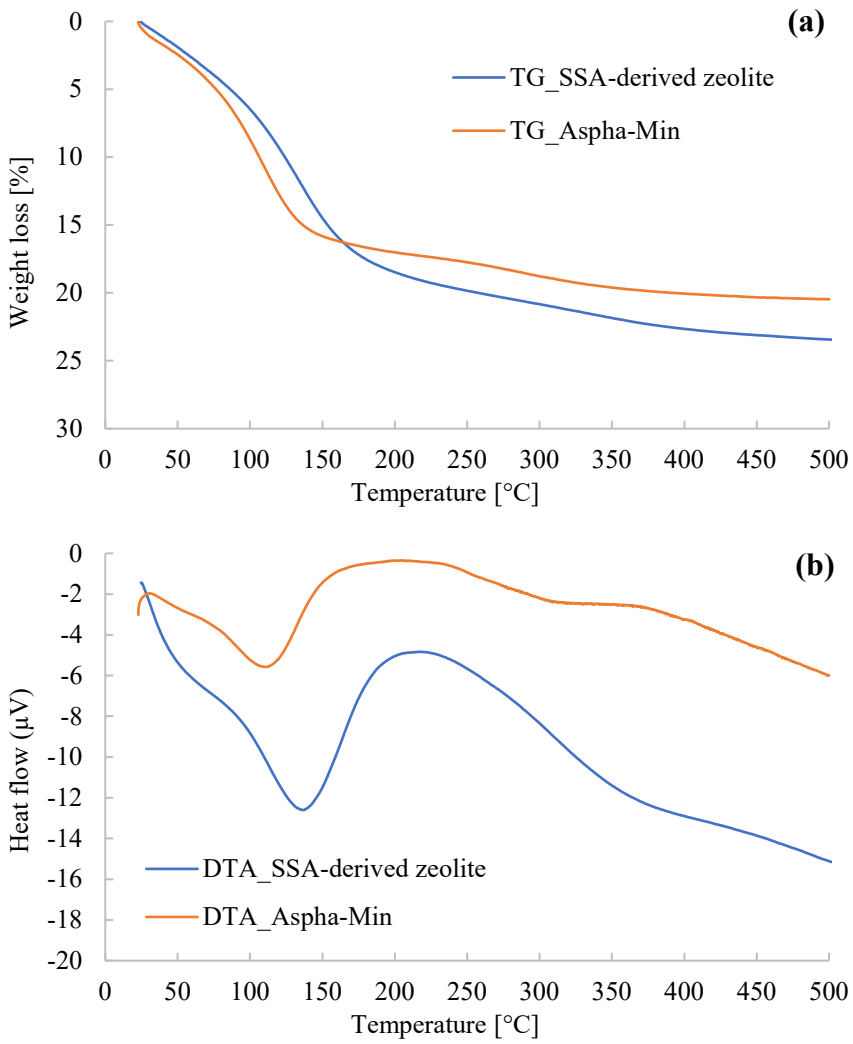

Fig. 4. (a) weight loss and (b) heat flow of SSA-derived zeolite and Aspha-min

3.2. Indirect tensile stiffness modulus of HMA and WMA mixtures

The ITSM test results are shown in **Fig. 5**. The indirect stiffness moduli of unaged HMA, WMAZ, and WMAA were 2,371 MPa, 2,018 MPa, and 2,148 MPa, respectively. It can be observed that the WMA mixtures showed lower values in stiffness modulus than the HMA mixture before aging. This was expected because the WMA mixtures had undergone considerably lower aging during manufacturing due to the 25 ºC lower production temperature. The WMAZ mixture showed the lowest stiffness modulus that was 15% lower than that of the HMA mixture and 6% lower than that of the WMAA mixture, which is helpful for cracking resistance at intermediate temperatures. After aging, the stiffness moduli of the WMA mixtures were slightly lower than the HMA mixture, but no significant difference was observed. The indirect stiffness moduli of aged HMA, WMAZ, and WMAA were 3,398 MPa, 3,300 MPa, and 3,367 MPa, respectively. The HMA mixture had the highest stiffness modulus which was 3%

higher than the WMAZ mixture and 1% higher than the WMAA mixture. This indicated that the lowered manufacturing temperature of WMA mixtures provides insignificant effects on their long-term cracking resistance. It was noticed that the WMAA has a slightly higher stiffness modulus compared to the WMAZ in both unaged and aged states. The filler effect may explain the discrepancies in their stiffness moduli. As both SSA-derived zeolite and Asphamin are crystalline microporous hydrated aluminosilicates, after releasing the crystal water, residual dehydrated aluminosilicates stay in the asphalt mixture and act as fillers. It was found that Asphamin has lower crystal water content than SSA-derived zeolite. Thus, when using the same application dosage, Asphamin was expected to have a higher number of fine aluminosilicates that stayed in the asphalt mixture as fillers after foaming completed, which results in the slightly higher stiffness modulus of the WMAA compared to the WMAZ (Abbas et al., 2005; Baskara et al., 2019). Moreover, it was found that asphalt mixtures may exhibit lower stiffness modulus when finer fillers are used (Muniandy and Aburkaba, 2011). This may be another reason that the WMAZ presents a lower stiffness modulus compared to the WMAA as the grain size of SSA-derived zeolite is smaller than Asphamin.

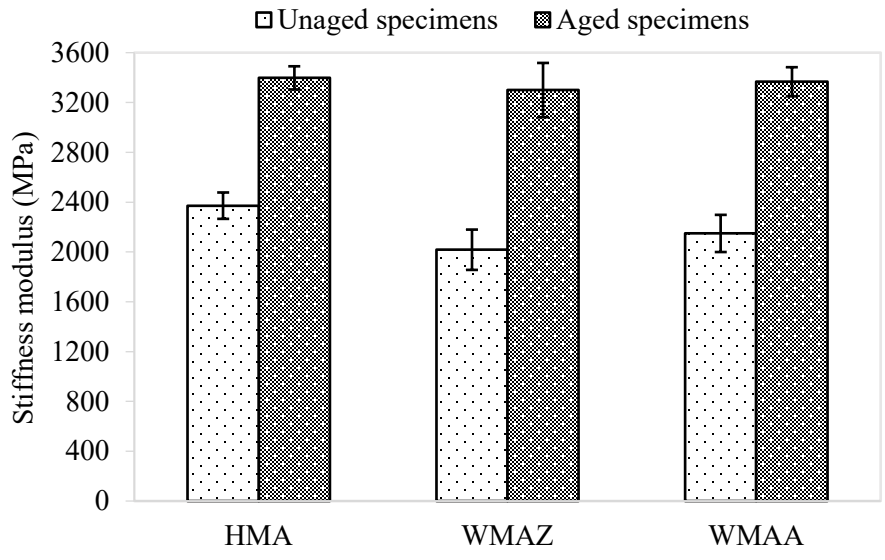

Fig. 5. Results of the ITSM tests of HMA and WMA mixtures before and after aging

3.3. Fatigue performance of HMA and WMA mixtures

The fatigue tests were conducted over an initial tensile strain range of 100 με to 400 με, and the resultant fatigue life of the tested material shall fall within a range between 10^3 and 10^6 per number of load applications. The conventional failure criterion N_{f50} was employed for estimating the fatigue life of the test specimens. **Fig. 6.** shows the fatigue life versus the initial strain of the HMA and WMA mixtures. The least-squares regression relationship was fitted to

the data of the initial strain as an independent variable and the data of the number of load applications of the fracture life as a dependent variable according to Equation 1:

$$N_f = k \times \left(\frac{1}{\varepsilon_0}\right)^n \quad (1)$$

where N_f is the number of load applications until fracture; k, n are material constants; and ε_0 is the initial tensile strain in με.

It can be observed that the HMA mixture and WMA mixtures had very similar fatigue lives in the log-scale diagram. The results suggested that the fatigue performances of the three mixtures are very close to each other. The fatigue lives of the WMA mixtures were slightly lower than the HMA mixture in high strains. Among the three mixtures, the WMAA mixture had the lowest and the HMA mixture had the highest fatigue life in high strains. There was no obvious difference in the fatigue life of the HMA mixture and the WMA mixtures in middle strains. In low strains, the WMAA mixture showed the highest fatigue life. **Table 5** presents the parameters of the regressional fatigue lines, as well as the predicted fatigue lives corresponding to the strains of 100 με, 200 με, and 400 με, respectively. The predicted fatigue lives corresponding to the high stain (400 με) for HMA, WMAZ, and WMAA were 3,170, 3,044, and 2,878, respectively. This suggested that the HMA mixture has better resistance to heavy good vehicles than the WMA mixtures. The predicted fatigue lives corresponding to the middle strain (200 με) for both WMA mixtures were 2% lower than that of the HMA mixture. The predicted fatigue life corresponding to the low strain (100 με) for the WMAA mixture was 526,045, which was 6% higher than those of the other two mixtures. The results indicated that WMA mixtures have slightly lower fatigue resistance at high stain levels and slightly better fatigue resistance at low strain levels. But overall, the fatigue resistances of the three mixtures are close to each other.

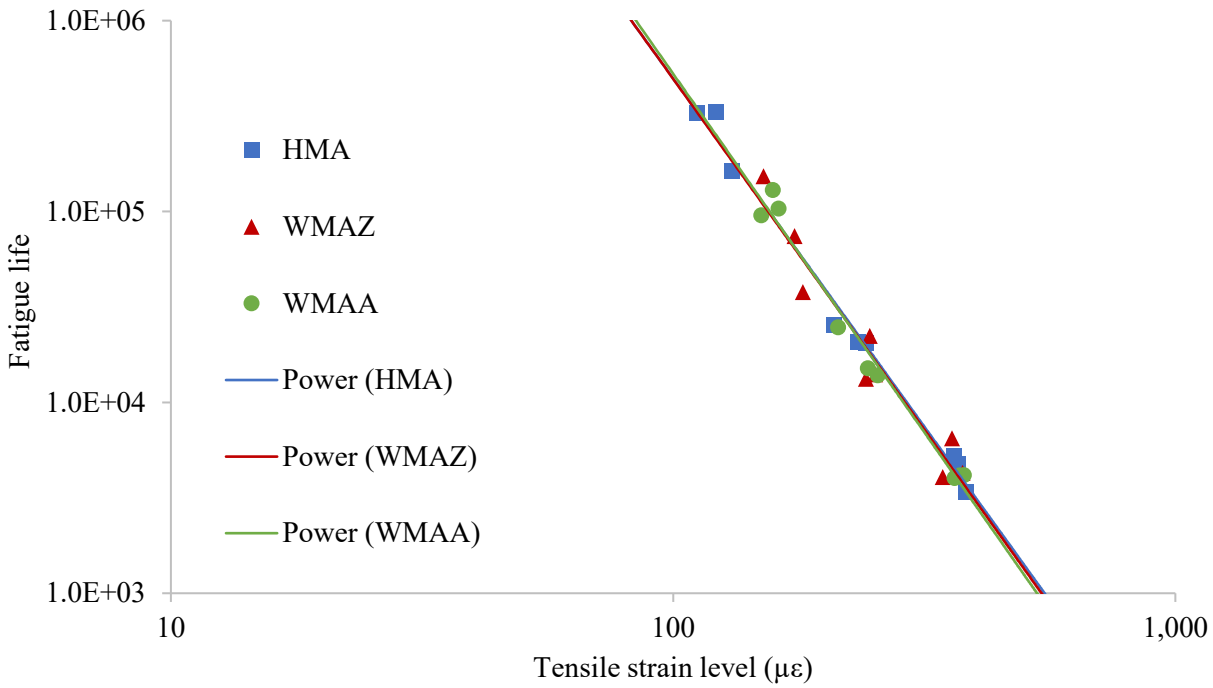

Fig. 6. Fatigue life versus initial strain for HMA and WMA mixtures

Table 5 Parameters of the fatigue lines and the predicted fatigue lives at different strains

Mixture	Parameter			Predicted fatigue life		
	k	n	R^2	cycles @ 100 με	cycles @ 200 με	cycles @ 400 με
HMA	9.790E+12	3.647	0.990	497,488	39,712	3,170
WMAZ	1.105E+13	3.674	0.943	495,864	38,849	3,044
WMAA	1.718E+13	3.757	0.981	526,045	38,909	2,878

3.4. Susceptibility to moisture damage of HMA and WMA mixtures

The effects of moisture on the WMA mixtures were investigated by measuring the tensile strength ratio between the mixtures with the freeze-thaw cycle conditioning, and the mixtures without the freeze-thaw cycle conditioning. The moisture susceptibility of the HMA mixture was also investigated for comparison purposes. **Fig. 7.** shows the results of the moisture susceptibility tests. The results indicated that the WMA mixtures had slightly higher strengths than the HMA mixture. The dry strengths of the HMA, WMAZ, and WMAA were 9.6 kN, 9.8kN, and 9.7 kN, respectively. After the freeze-thaw conditioning, there was an obvious decrease in the indirect tensile strength for all mixtures. The wet strengths of the HMA, WMAZ, and WMAA were 7.8 kN, 8.1 kN, and 8.0 kN, respectively. It can be observed that the WMAZ mixture had the highest strength both before and after conditioning, but the difference is not significant. The tensile strength ratios for HMA, WMAZ, and WMAA were 80.87%, 82.71%, and 82.14%, respectively.

The results suggested that there is no specific concern about the moisture susceptibility of WMA mixtures prepared by using SSA-derived zeolite as the additive. The usage of lime might be one of the main contributing factors to the satisfactory moisture damage resistance of all the mixtures. The discrepancies in the micro-properties of SSA-derived zeolite and commercial zeolite Asphamin may be the reason that leads to the higher tensile strengths of the WMAZ both dry and wet compared to the WMAA. It was found that SSA-derived zeolite has a higher Si/Al ratio, more divalent cations, and smaller gran sizes compared to Asphamin, which results in higher water binding ability and stronger water-binding force of SSA-derived zeolite. It was observed that SSA-derived zeolite can release water more gradually, which results in a better foaming effect. Therefore, the better foaming effect and aggregate coating improved the strength development of the WMAZ compared to the WMAA.

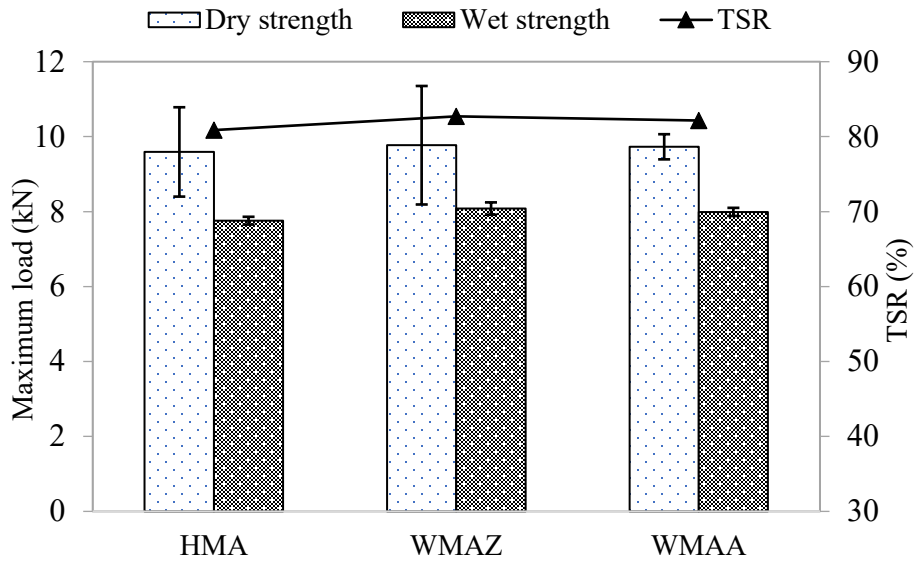

Fig. 7. Results of the tensile strengths of HMA and WMA mixtures

3.5. Rutting resistance of HMA and WMA mixtures

From the Hamburg wheel-tracking test, the following three performance parameters of the testing specimens are commonly obtained: a) creep slope: the depth of rutting per loading pass in the creep stage, which indicates the rutting resistance; b) stripping slope: the depth of rutting per loading pass in the stripping stage, which indicates the resistance to moisture damage; and c) stripping inflection point (SIP): the number of passes at which the regression lines of the creep stage and the stripping stage intersects, indicating the start of moisture damage.

Fig. 8. shows the results of the Hamburg wheel-tracking tests of HMA and WMA mixtures at two different temperatures. The values corresponding to the creep slope and the maximum rut depth are given in **Table 6**. It was noticed that the stripping slope and the SIP were not observed

in the results, indicating the good moisture damage resistance potential of the testing mixtures, which is consistent with the results of the moisture susceptibility tests. From **Fig. 8 (a).**, it can be seen that the HMA mixture had the lowest rut depth of 3.20 mm after 20,000 cycles of loading at 50 ºC, while the values for the WMA mixtures were higher and the WMAA mixture had the highest rut depth of 3.92 mm. The results indicated that the HMA mixture provided better rutting resistance than the WMA mixtures. This was expected because the production temperatures of WMA mixtures were considerably lower than the HMA mixture. The rutting potential increases with the decrease of mixture production temperatures, which is related to the decreased aging of asphalt binder in the WMA mixtures (Bennert et al., 2011). The results also suggested that the WMAZ mixture had better rutting resistance than the WMAA mixture. The maximum rut depth of the WMAZ mixture was 5% lower than that of the WMAA mixture. For asphalt mixtures with a PG-76 binder, it is common to allow for a maximum rut depth of 12.7mm (0.5 in.) at 20,000 passes in Hamburg wheel-tracking test (Yildirim et al., 2007). Thus, it can be noted that the measured wheel-tracking depths of both WMA mixtures satisfied the recommended requirement, although they were slightly larger than that of the HMA mixture.

To understand their rutting resistances in a harsher environment, the Hamburg wheel-tracking rut depths of the three mixtures were also measured at a higher temperature of 60 ºC, as presented in **Fig. 8 (b)**. It is obvious that the rut depths of all mixtures were significantly increased due to the increased testing temperature, but the ranking followed the same trend as that at 50 ºC. It was also interesting to notice that even though the test temperature had been increased by 10 ºC, the maximum rut depths of the three mixtures were still smaller than 12.7 mm. These results suggested that all the three mixtures had good rutting resistance even in the case of extremely hot weather.

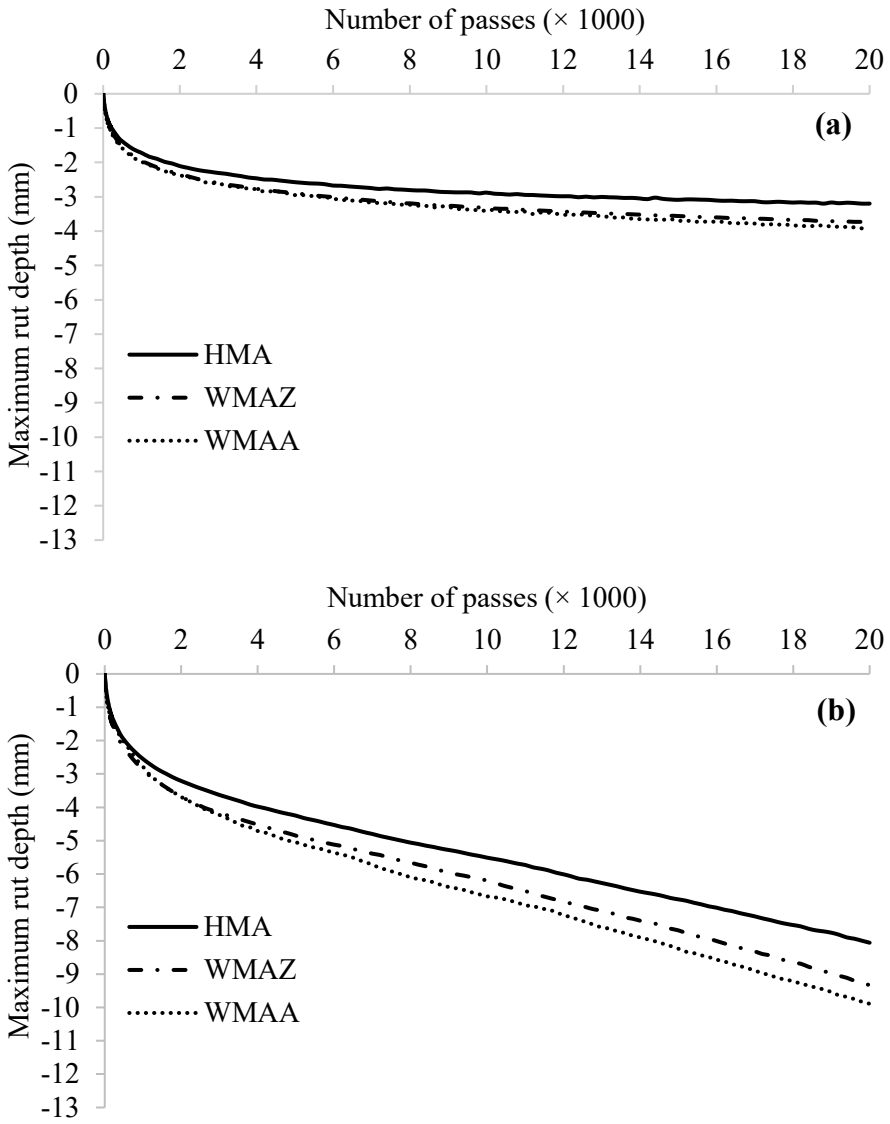

Fig. 8. Hamburg wheel-tracking curves of HMA and WMA mixtures at: (a) 50 ºC; and (b) 60 ºC

Table 6 Summary of the values of creep slope and the maximum rut depth

Mixture	Test temperature (ºC)	Creep slope (mm/ 1000 passes)	Maximum rut depth (mm)
HMA	50	0.061	3.20
WMAZ		0.078	3.74
WMAA		0.086	3.92
HMA	60	0.269	8.06
WMAZ		0.314	9.33
WMAA		0.344	9.89

3.6. Cost-benefit analysis

Fig. 9. illustrates the evaluated cost-benefit results for producing 1 kg SSA-derived zeolite. Based on the cost inventory, the total cost for the recycling process is $0.87/kg. The advantage in the economy of the SSA recycling could be observed, compared with the cost of $1.35/kg for commercial zeolite additive (Sukhija and Saboo, 2020). The large proportion of $NaAlO_2$ enables the price of $NaAlO_2$ to become the most influential factor in the overall synthesis cost. In addition, due to the varied costs of mineral filler, the benefit from the by-product ranged from $0.02-$0.12 when producing 1 kg zeolite. As the fixed cost of SSA-derived zeolite is calculated based on the market price of the raw materials and energy consumption collected under the laboratory conditions, the cost is expected to be reduced under the mass production when facing the market. Although this evaluation may be lower than its potential market price as it did not consider the rate of return, it provides the initial insight into the benefit of cost-efficiency of SSA-derived zeolite.

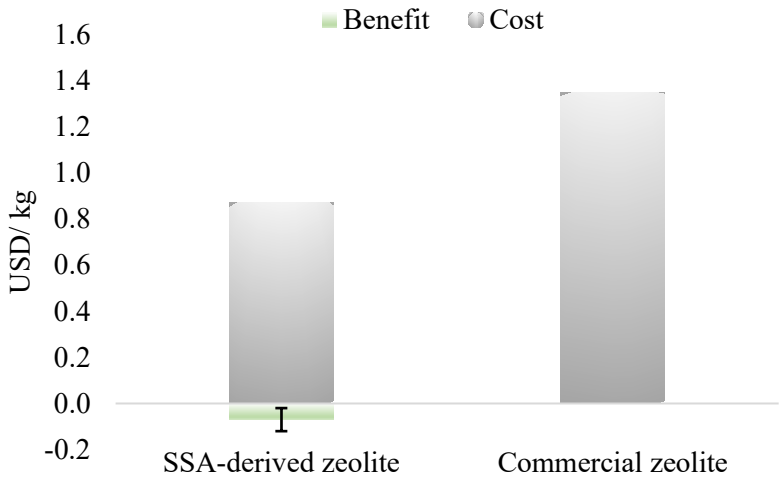

Fig. 9. Cost-benefit results for producing 1kg SSA-derived zeolite

4. Summary and Findings

In this study, synthetic zeolite was first derived from SSA and its chemical properties were characterized and compared with those of the commercial WMA additive, Aspha-min. Then, two WMA mixtures (WMAZ & WMAA) were produced by using SSA-derived zeolite and Aspha-min as additives, respectively. Finally, comprehensive laboratory tests were conducted to study the performance properties of the produced WMA mixtures in comparison with an HMA mixture with the same gradation, followed by a cost-benefit analysis. Based on the outcomes of this study, the following findings were obtained:

- The SSA-derived zeolite was characterized to be pure zeolite A which can release approximately 20% crystal water gradually from 70 ºC to 200 ºC. It has a similar crystalline structure as the commercial zeolite, Aspha-min, but with a smaller grain size. Compared with

Aspha-min, the SSA-derived zeolite contained a relatively larger percentage of crystal water and provided a more gradual release of crystal water when heated.

- The stiffness modulus of the WMAZ mixture was 15% lower than the HMA mixture and 6% lower than the WMAA mixture. Such differences in the stiffness modulus became very subtle after aging. The produced HMA and WMA mixtures showed very similar resistances to fatigue cracking, and there was no significant difference observed in their fatigue lives.
- The WMAZ mixture showed slightly higher strengths compared to the HMA and WMAA mixtures. The tensile strength ratios for WMAZ, HMA, and WMAA were 82.71%, 80.87%, and 82.14%, respectively, indicating similar good resistance to moisture damage of all mixtures.
- The rutting resistances of all three mixtures were satisfactory, although the two WMA mixtures showed larger rut depth than the HMA mixture, which was mainly caused by the decreased aging of the WMA mixtures during production. Compared with WMAA, WMAZ showed slightly better rutting resistance.
- SSA-derived zeolite can reduce the 35.6%-50% of the cost per kilogram, which shows its advantages in the economy compared with commercial zeolite products based on the data collected in this study.

To summarize, the overall engineering performance of the WMA mixture with SSA-derived zeolite additive was similar to the HMA mixture and superior to the WMA mixture with the commercial foaming additive in terms of cracking resistance, fatigue resistance, and moisture susceptibility. It is anticipated that the utilization of such SSA-derived zeolite materials could open a new outlet for the economical disposal of waste products currently landfilled and help relieve the strain of disposal. However, it should be noted that the findings of this study were based on the results of laboratory tests on one type of asphalt mixture. Laboratory tests on different asphalt mixtures and field trials are recommended in the future to further verify the performance of the SSA-derived zeolite as a WMA additive.

Acknowledgments

The authors would like to acknowledge the financial supports from the Hong Kong Environment and Conservation Fund under Grant number ECF 2015-61.

References

AASHTO M320-10, 2013. Standard specification for performance-graded asphalt binder. Am. Assoc. S. Highw. Trans. Off. Washington, D.C., United States.

AASHTO R30-02, 2010. Standard practice for mixture conditioning of hot mix asphalt (HMA). Am. Assoc. S. Highw. Trans. Off. Washington, D.C., United States.

AASHTO T324-11, 2013. Hamburg wheel-track testing of compacted hot mix asphalt (HMA). Assoc. S. Highw. Trans. Off. Washington, D.C., United States.

Abbas, A., Masad, E., Papagiannakis, T., Shenoy, A., 2005. Modelling asphalt mastic stiffness using discrete element analysis and micromechanics-based models. Int. J. Pavement Eng. 6(2), 137-146. https://doi.org/10.1080/10298430500159040.

Afzal, M., Yasmeen, G., Saleem, M., Butt, P.K., Khattak, A.K., Afzal, J., 2000. TG and DTA study of the thermal dehydration of metal-exchanged zeolite-4A samples. J. Therm. Analysis Calorim. 62, 721-727. https://doi.org/10.1023/a:1026725509732.

Anderson, M., Skerratt, R. G., 2003. Variability study of incinerated sewage sludge ash in relation to future use in ceramic brick manufacture. Br. Ceram. Trans. 102(3), 109-113. https://doi.org/10.1179/096797803225001614.

ASTM D4867-09, 2014. Standard test method for effect of moisture on asphalt concrete paving mixtures. Am. Soc. Test. Mater. Int. Pennsylvania, United States.

Baskara, G. M. B., Ahyudanari, E., Thanaya, I. N. A., 2019. Analysis of Stiffness Modulus of Asphalt Concrete Mixture by Using Artificial Aggregates. J. Tek. ITS. 8(2), F81-F85.

Benassi, L., Zanoletti, A., Depero, L.E., Bontempi, E., 2019. Sewage sludge ash recovery as valuable raw material for chemical stabilization of leachable heavy metals. J. Environ. Manag. 245, 464-470. https://doi.org/10.1016/j.jenvman.2019.05.104.

Bennert, T., Maher, A., Sauber, R., 2011. Influence of production temperature and aggregate moisture content on the initial performance of warm-mix asphalt. Transp. Res. Rec.: J. Transp. Res. Board. 2208 (1), 97-107. https://doi.org/10.3141/2208-13.

BS DD 213, 1993. Method for determination of the indirect tensile stiffness modulus of bituminous mixtures. Br. Stand. Inst. London, U.K.

BS EN 12697-24, 2012. Bituminous mixtures – test methods for hot mix asphalt part 24: resistance to fatigue. Br. Stand. Inst. London, U.K.

Capitão, S. D., Picado-Santos, L. G., Martinho, F., 2012. Pavement engineering materials: review on the use of warm-mix asphalt. Constr. Build. Mater. 36, 1016-1024. https://doi.org/10.1016/j.conbuildmat.2012.06.038.

Cardoso, A.M., Horn, M.B., Ferret, L.S., Azevedo, C.M.N., Pires, M., 2015. Integrated synthesis of zeolites 4A and Na-P1 using coal fly ash for application in the formulation of detergents and swine wastewater treatment. J. Hazard. Mater. 287, 69-77. https://doi.org/10.1016/j.jhazmat.2015.01.042.

Collins, F., Rozhkovskaya, A., Outram, J. G., Millar, G. J., 2020. A critical review of waste resources, synthesis, and applications for Zeolite LTA. Microporous Mesoporous Mater. 291, 109667. https://doi.org/10.1016/j.micromeso.2019.109667.

Cyr, M., Coutand, M., Clastres, P., 2007. Technological and environmental behavior of sewage sludge ash (SSA) in cement-based materials. Cem. Concr. 37(8), 1278-1289. https://doi.org/10.1016/j.cemconres.2007.04.003.

de Angelis Curtis, S., Curini, R., D'Ascenzo, G., Sagone, F., Fachin, S., Bocca, A., 1999. Grana Padano cheese: thermoanalytical techniques applied to the study of ripening. Food Chem. 66(3), 375-380. https://doi.org/10.1016/S0308-8146(99)00073-4.

Donatello, S., Cheeseman, C. R., 2013. Recycling and recovery routes for incinerated sewage sludge ash (ISSA): A review. Waste Manag. 33(11), 2328-2340. https://doi.org/10.1016/j.wasman.2013.05.024.

Duan, Y., Li, J., Yang, X., Hu, L., Wang, Z., Liu, Y., Wang, C., 2008. Kinetic analysis on the non-isothermal dehydration by integral master-plots method and TG–FTIR study of zinc acetate dihydrate. J. Anal. Appl. Pyrolysis. 83(1), 1-6. https://doi.org/10.1016/j.jaap.2008.05.001.

Hasan, M.R.M., You, Z., Porter, D., Goh, S.W., 2015. Laboratory moisture susceptibility evaluation of wma under possible field conditions. Constr. Build. Mater. 101, 57-64. https://doi.org/10.1016/j.conbuildmat.2015.10.004.

Jiang, J., Li, Y., Zhang, Y., Bahia, H.U., 2020. Distribution of mortar film thickness and its relationship to mixture cracking resistance. Int. J. Pavement Eng. https://doi.org/10.1080/10298436.2020.1774767.

Kheradmand, B., Muniandy, R., Hua, L.T., Yunus, R.B., Solouki, A., 2014. An overview of the emerging warm mix asphalt technology. Int. J. Pavement Eng. 15 (1), 79-94. https://doi.org/10.1080/10298436.2013.839791.

Kim, J.K., Lee, H.D., 2009. Effects of step change of heating source on synthesis of zeolite 4A from coal fly ash. J. Ind. Eng. Chem. 15, 736-742. https://doi.org/10.1016/j.jiec.2009.09.055.

Kristjánsdóttir, Ó., Muench, S.T., Michael, L., Burke, G., 2007. Assessing potential for warm-mix asphalt technology adoption. Transp. Res. Rec.: J. Transp. Res. Board. 2040, 91-99. https://doi.org/10.3141/2040-10.

Lam, C. M., Lee, P. H., Hsu, S. C., 2015. Eco-efficiency analysis of sludge treatment scenarios in urban cities: the case of Hong Kong. J. Clean. Prod. 112, 3028-3039. https://doi.org/10.1016/j.jclepro.2015.10.125.

Leng, Z., Gamez, A., Al-Qadi, I. L., 2014. Mechanical property characterization of warm-mix asphalt prepared with chemical additives. J. Mater. Civil. Eng. 26 (2), 304-311. https://doi.org/10.1061/(ASCE)MT.1943-5533.0000810.

Li, R., Leng, Z., Wang, Y., Zou, F., 2020. Characterization and correlation analysis of mechanical properties and electrical resistance of asphalt emulsion cold-mix asphalt. Constr. Build. Mater. 263, 119974. https://doi.org/10.1016/j.conbuildmat.2020.119974.

Mahieux, P. Y., Aubert, J. E., Cyr, M., Coutand, M., Husson, B., 2010. Quantitative mineralogical composition of complex mineral wastes–Contribution of the Rietveld method. Waste Manag. 30(3), 378-388. https://doi.org/10.1016/j.wasman.2009.10.023.

Middleton, B., Forfylow, R., 2009. Evaluation of warm-mix asphalt produced with the double barrel green process. Transp. Res. Rec.: J. Transp. Res. Board. 2126 (1), 19-26. https://doi.org/10.3141/2126-03.

Muniandy, R., Aburkaba, E., 2011. The effect of type and particle size of industrial wastes filler on Indirect Tensile Stiffness and Fatigue performance of Stone Mastic Asphalt Mixtures. Aust. J. Basic & Appl. Sci. 5(11), 297-308.

Murayama, N., Yamamoto, H., Shibata, J., 2002. Mechanism of zeolite synthesis from coal fly ash by alkali hydrothermal reaction. Int. J. Min. Process 64, 1-17. https://doi.org/10.1016/S0301-7516(01)00046-1.

Qian, T., Li, J., 2015. Synthesis of Na-A zeolite from coal gangue with the in-situ crystallization technique. Adv. Powder Technol. 26(1), 98-104. https://doi.org/10.1016/j.apt.2014.08.010.

Rios, C.A., Williams, C.D., Fullen, M.A., 2009. Nucleation and growth history of zeolite LTA synthesized from kaolinite by two different methods. Appl. Clay Sci. 42, 446-454. https://doi.org/10.1016/j.clay.2008.05.006.

Research and Development Division, Highways Department, 2020. Guidance notes: application of polymer modified stone mastic asphalt, RD/GN/038A. https://www.hyd.gov.hk/en/publications_and_publicity/publications/technical_document/guidance_notes/index.html (accessed 25 July 2020).

Rubio, M. C., Martínez, G., Baena, L., Moreno, F., 2012. Warm mix asphalt: an overview. J. Clean. Prod. 24, 76-84. https://doi.org/10.1016/j.jclepro.2011.11.053.

Saldo, J., Sendra, E., & Guamis, B., 2002. Changes in water binding in high-pressure treated cheese, measured by TGA (thermogravimetrical analysis). Innov Food Sci Emerg Technol. 3(3), 203-207. https://doi.org/10.1016/S1466-8564(02)00047-4.

Sengoz, B., Topal, A., Gorkem, C., 2013. Evaluation of natural zeolite as warm mix asphalt additive and its comparison with other warm mix additives. Constr. Build. Mater. 43, 242-252. https://doi.org/10.1016/j.conbuildmat.2013.02.026.

Statistics Unit, Environmental Protection Department, 2020. Monitoring of solid waste in Hong Kong: waste statistics for 2018. https://www.wastereduction.gov.hk/en/assistancewizard/waste_red_sat.htm (accessed 25 July 2020).

Sukhija, M., Saboo, N., 2020. A comprehensive review of warm mix asphalt mixtures-laboratory to field. Constr. Build. Mater. 274, 121781. https://doi.org/10.1016/j.conbuildmat.2020.121781.

568 Valdes-Vidal, G., Calabi-Floody, A., Sanchez-Alonso, E., 2018. Performance evaluation of
569 warm mix asphalt involving natural zeolite and reclaimed asphalt pavement (RAP) for
570 sustainable pavement construction. Constr. Build. Mater. 174, 576-585.
571 https://doi.org/10.1016/j.conbuildmat.2018.04.149.
572 Wang, D., Liang, X., Li, D., Liang, H., Yu, H., 2018b. Study on mechanics-based cracking
573 resistance of semiflexible pavement materials. Adv. Mater. Sci. Eng.
574 https://doi.org/10.1155/2018/8252347.
575 Wang, L., Zou, F., Fang, X., Tsang, D.C.W., Poon, C.S., Leng, Z., Baek, K., 2018a. A novel type
576 of controlled low strength material derived from alum sludge and green materials. Constr.
577 Build. Mater. 165, 792-800. https://doi.org/10.1016/j.conbuildmat.2018.01.078.
578 Wiebusch, B., Seyfried, C. F., 1997. Utilization of sewage sludge ashes in the brick and tile
579 industry. Water Sci. Technol. 36(11), 251-258. https://doi.org/10.1016/S0273-
580 1223(97)00688-4.
581 Woszuk A., Franus, W., 2017. A review of the application of zeolite materials in warm mix
582 asphalt technologies. Appl. Sci. 7(3), 293-307. https://doi.org/10.3390/app7030293.
583 Woszuk, A., Zofka, A., Bandura, L., Franus, W., 2017. Effect of zeolite properties on asphalt
584 foaming. Constr Build Mater. 139, 247-255.
585 https://doi.org/10.1016/j.conbuildmat.2017.02.054.
586 Xiao, F., Punith, V., Putman, B., Amirkhanian, S.N., 2011. Utilization of foaming technology in
587 warm-mix-asphalt mixtures containing moist aggregates. J. Mater. Civil. Eng. 23 (9), 1328-
588 1337. https://doi.org/10.1061/(ASCE)MT.1943-5533.0000297.
589 Xu, S., Xiao, F., Amirkhanian, S., Singh, D., 2017. Moisture characteristics of mixtures with
590 warm mix asphalt technologies – a review. Constr. Build. Mater. 142, 148-161.
591 https://doi.org/10.1016/j.conbuildmat.2017.03.069.
592 Yildirim, Y., Jayawickrama, P.W., Hossain, M.S., Alhabshi, A., Yildirim, C., Smit, A.F., Little,
593 D., 2007. Hamburg wheel-tracking database analysis. Publication FHWA/TX-05/0-1707-7.
594 Tex. Dep. Transp. Texas, United States.
595 Yu, H., Leng, Z., Dong, Z., Tan, Z., Guo, F., Yan, J., 2018. Workability and mechanical property
596 characterization of asphalt rubber mixtures modified with various warm mix asphalt
597 additives. Constr. Build. Mater. 175, 392-401.
598 https://doi.org/10.1016/j.conbuildmat.2018.04.218.
599 Zhang, Y., Leng, Z., Zou, F., Wang, L., Chen, S.S., Tsang, D.C.W., 2018. Synthesis of zeolite a
600 using sewage sludge ash for application in warm mix asphalt. J. Clean. Prod. 172, 686-695.
601 https://doi.org/10.1016/j.jclepro.2017.10.005.
602 Zhou, Y., Li, J., Lu, J., Cheeseman, C., Poon, C.S., 2020. Recycling incinerated sewage sludge
603 ash (ISSA) as a cementitious binder by lime activation. J. Clean. Prod. 244, 118856.
604 https://doi.org/10.1016/j.jclepro.2019